JACS
JOURNAL OF THE AMERICAN CHEMICAL SOCIETY
Article
pubs.acs.org/JACS

D_{2d}(23)-C_{84} versus Sc_2C_2@D_{2d}(23)-C_{84}: Impact of Endohedral Sc_2C_2 Doping on Chemical Reactivity in the Photolysis of Diazirine

Michio Yamada,[†] Yukiko Tanabe,[‡] Jing-Shuang Dang,[§,¶] Satoru Sato,[‡] Naomi Mizorogi,[‡] Makoto Hachiya,[‡] Mitsuaki Suzuki,[†,△] Tsuneyuki Abe,[‡] Hiroki Kurihara,[‡] Yutaka Maeda,[†] Xiang Zhao,[§] Yongfu Lian,[‡,∥] Shigeru Nagase,[⊥] and Takeshi Akasaka*[,†,‡,#]

[†]Department of Chemistry, Tokyo Gakugei University, Tokyo 184-8501, Japan

[‡]Life Science Center of Tsukuba Advanced Research Alliance, University of Tsukuba, Ibaraki 305-8577, Japan

[§]Institute for Chemical Physics & Department of Chemistry, State Key Laboratory of Electrical Insulation and Power Equipment, Xi'an Jiaotong University, Xi'an 710049, China

[∥]Key Laboratory of Functional Inorganic Material Chemistry, Ministry of Education, School of Chemistry and Materials Science, Heilongjiang University, Harbin 150080, China

[⊥]Fukui Institute for Fundamental Chemistry, Kyoto University, Kyoto 606-8103, Japan

[#]Foundation for Advancement of International Science, Ibaraki 305-0821, Japan

Supporting Information

ABSTRACT: We compared the chemical reactivity of D_{2d}(23)-C_{84} and that of Sc_2C_2@D_{2d}(23)-C_{84}, both having the same carbon cage geometry, in the photolysis of 2-adamantane-2,3′-[3*H*]-diazirine, to clarify metal-atom doping effects on the chemical reactivity of the carbon cage. Experimental and computational studies have revealed that the chemical reactivity of the D_{2d}(23)-C_{84} carbon cage is altered drastically by endohedral Sc_2C_2 doping. The reaction of empty D_{2d}(23)-C_{84} with the diazirine under photoirradiation yields two adamantylidene (Ad) adducts. NMR spectroscopic studies revealed that the major Ad monoadduct (C_{84}(Ad)-A) has a fulleroid structure and that the minor Ad monoadduct (C_{84}(Ad)-B) has a methanofullerene structure. The latter was also characterized using X-ray crystallography. C_{84}(Ad)-A is stable under photoirradiation, but it interconverted to C_{84}(Ad)-B by heating at 80 °C. In contrast, the reaction of endohedral Sc_2C_2@D_{2d}(23)-C_{84} with diazirine under photoirradiation affords four Ad monoadducts (Sc_2C_2@C_{84}(Ad)-A, Sc_2C_2@C_{84}(Ad)-B, Sc_2C_2@C_{84}(Ad)-C, and Sc_2C_2@C_{84}(Ad)-D). The structure of Sc_2C_2@C_{84}(Ad)-C was characterized using X-ray crystallography. Thermal interconversion of Sc_2C_2@C_{84}(Ad)-A and Sc_2C_2@C_{84}(Ad)-B to Sc_2C_2@C_{84}(Ad)-C was also observed. The reaction mechanisms of the Ad addition and thermal interconversion were elucidated from theoretical calculations. Calculation results suggest that C_{84}(Ad)-B and Sc_2C_2@C_{84}(Ad)-C are thermodynamically favorable products. Their different chemical reactivities derive from Sc_2C_2 doping, which raises the HOMO and LUMO levels of the D_{2d}(23)-C_{84} carbon cage.

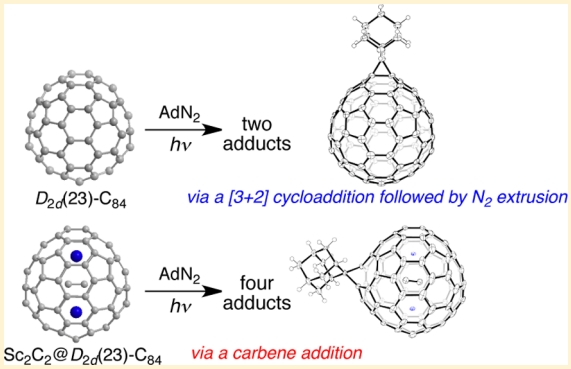

INTRODUCTION

Encapsulation of metal atoms or metal-containing clusters in fullerene cages provides hybrid molecules known as endohedral metallofullerenes (EMFs).[1] Recent progress has revealed that the chemical reactivity of EMFs differs greatly from that of empty fullerenes and that it is strongly dependent on the encaged metal species. For instance, M@C_{2v}(9)-C_{82} (M = La, Ce, Pr, Gd, and Y) and M_2@I_h(7)-C_{80} (M = La and Ce) undergo both photochemical and thermal reactions with disilirane to form bis-silylated adducts, whereas the reactions of empty fullerenes (C_{60}, C_{70}, C_{76}, and D_2(22)-C_{84}) and Sc_3N@I_h(7)-C_{80} with disilirane are suppressed under thermal conditions.[2] Akasaka et al. reported that retro-reaction of a Diels–Alder adduct, La@C_{2v}(9)-C_{82}(Cp) (Cp = cyclopentadiene), proceeded much faster than that of C_{60}(Cp).[3] Accordingly, Dorn et al. developed a nonchromatographic purification protocol for isolating M_3N@C_{80} (M = Sc, Gd, Er, Lu, etc.) from soot extracts containing empty fullerenes and other EMFs by taking advantage of its kinetic chemical stability with respect to the Diels–Alder reaction with Cp-functionalized resins.[4] These differences in chemical reactivity between empty fullerenes and EMFs derive from the presence of intramolecular electron transfer from endohedral metal species

Received: October 17, 2016
Published: November 25, 2016

DOI: 10.1021/jacs.6b10751
J. Am. Chem. Soc. 2016, 138, 16523–16532

to the carbon cages, thereby drastically altering their electronic structures in EMFs. Nevertheless, how the metal encapsulation affects the chemical reactivity of the carbon cages in reactions is an issue that has remained unexplored.[5] An important difficulty in answering this question is the fact that almost no carbon cage of EMFs is available in its empty form. Such a situation results from the fact that endohedral metal-atom doping drastically alters the thermodynamic stability of the carbon cages. In this respect, the sole exception is the $D_{2d}(23)$-C_{84} carbon cage. To date, both empty $D_{2d}(23)$-C_{84}[6] and endohedral Sc_2C_2@$D_{2d}(23)$-C_{84}[7] are known to be stable and available in pristine forms (see Figure 1).

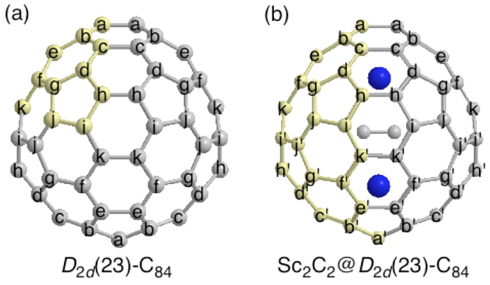

Figure 1. (a) Structure of $D_{2d}(23)$-C_{84}, where the 11 nonequivalent carbon atoms on the cage are labeled as a–k. (b) Structure of Sc_2C_2@$D_{2d}(23)$-C_{84}, where the 22 nonequivalent carbon atoms on the cage are labeled as a–k and a′–k′. Lowering of the molecular symmetry results from the Sc_2C_2 cluster placement because the C_2 unit is not parallel to the main C_2 axis.

Photolysis of diazirines generates carbenes and diazo intermediates, both of which are reactive to C_{60}.[8] Results show that adamantylidene (Ad) carbene reacts with a [6,6]-bond (bonds between two six-membered rings) of C_{60} via [2 + 1] cycloaddition to afford the [6,6]-closed methanofullerene ([6,6]-C_{60}(Ad)), whereas diazoadamantane reacts with one of the [5,6]-bonds (bonds between a five-membered ring and a six-membered ring) of C_{60} via [3 + 2] cycloaddition with subsequent N_2 extrusion from the pyrazoline intermediate to afford the [5,6]-open fulleroid ([5,6]-C_{60}(Ad)).[9] In fact, the photolysis of 2-adamantane-2,3′-[3*H*]-diazirine (**1**) in the presence of C_{60} yielded [6,6]-C_{60}(Ad) and [5,6]-C_{60}(Ad) in a 49:51 ratio, which shows good agreement with the formation ratio of Ad carbene and diazoadamantane ascertained from laser flash photolysis.[10] In that case, the C_{60}(Ad) derivatives, [6,6]-C_{60}(Ad) and [5,6]-C_{60}(Ad), do not mutually interconvert under the photolytic conditions. In this respect, C_{60} can act as a chemical probe for characterization of the photolytic pathway of diazirines.[11] However, Akasaka et al. found that La@$C_{2v}(9)$-C_{82} is reactive toward Ad carbene, but that it is not reactive toward diazoadamantane, for the photolysis of **1**.[2a,12] The regioselectivity in the Ad carbene addition to La@$C_{2v}(9)$-C_{82} is explainable by localization of the charge densities and the large *p*-orbital axis vector (POAV)[13] values on the carbon atoms near the encaged La atom, although the HOMO is delocalized over the C_{82} sphere. X-ray crystallographic analysis of the Ad monoadduct of La@$C_{2v}(9)$-C_{82} revealed that the electrophilic Ad carbene selectively bonded to one of the six most electron-rich strained carbon atoms. As described in this paper, we explore the chemical reactivity of $D_{2d}(23)$-C_{84} and that of Sc_2C_2@$D_{2d}(23)$-C_{84} in the photolysis of **1** to clarify how Sc_2C_2 doping affects the chemical reactivity of the $D_{2d}(23)$-C_{84} carbon cage.

RESULTS AND DISCUSSION

Reactivity of $D_{2d}(23)$-C_{84} and the Structure Determination of the Ad Adducts. Photoirradiation to a toluene solution of $D_{2d}(23)$-C_{84}, which we abbreviate as C_{84}, and an excess (47 equiv) of **1** at room temperature was conducted using a ultrahigh-pressure mercury-arc lamp (cutoff <350 nm). The reaction was monitored using analytical HPLC (Scheme 1). After irradiation for 90 s, 52% of C_{84} was consumed. Two

Scheme 1. Reaction of C_{84} with 1 under Photoirradiation

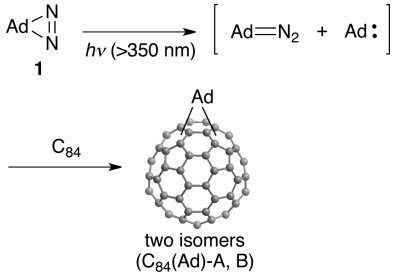

new peaks were observed. MALDI-TOF mass spectrometry revealed the products to be Ad monoadducts. Subsequent recycling HPLC separation afforded isolation of the two products (designated as C_{84}(Ad)-A for the major product and C_{84}(Ad)-B for the minor product). The conversion yields of C_{84}(Ad)-A and C_{84}(Ad)-B were estimated as 80% and 12% using the HPLC peak area.

The structure of C_{84}(Ad)-B was ascertained using single-crystal X-ray diffractometry (XRD). The X-ray structure shown in Figure 2 confirms that cyclopropanation occurred at the (a–

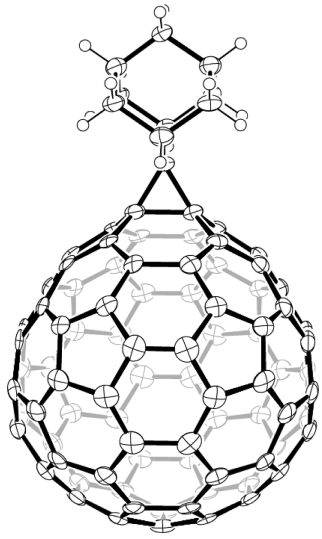

Figure 2. ORTEP drawing of C_{84}(Ad)-B ([6,6]-(a–a)-closed methanofullerene) with thermal ellipsoids shown at the 50% probability level for 90 K. Solvate molecules are omitted for clarity.

a) bond between the two six-membered rings on the C_{84} carbon cage (hereinafter the bond is designated as a [6,6]-(a–a) bond; labeling of carbon atoms in the C_{84} carbon cage is shown in Figure 1a). It is noteworthy that the site of addition in C_{84}(Ad)-B is similar to that reported for the addition of an iridium complex.[6d] The C–C distance between the cage carbons bonded to the Ad moiety was found to be 1.566 Å. Results show that C_{84}(Ad)-B has C_{2v} symmetry. The [6,6]-(a–

DOI: 10.1021/jacs.6b10751
J. Am. Chem. Soc. 2016, 138, 16523–16532

a)-closed methanofullerene structure of C_{84}(Ad)-B was also characterized using ^{1}H and ^{13}C NMR spectroscopy, which showed that NMR resonance patterns are consistent with the X-ray structure. The ^{13}C NMR spectrum exhibits 7 signals for the Ad skeleton, 19 signals out of 21 expected ones for the C_{84} cage at the sp^2 carbon region of 134−152 ppm, and 1 signal for the bonded sp^3 cage carbon at 68.86 ppm.

For C_{84}(Ad)-A, all attempts to grow single crystals were unsuccessful. However, the ^{1}H and ^{13}C NMR spectra suggest that C_{84}(Ad)-A has C_1 symmetry. Particularly, the ^{13}C NMR spectrum exhibits 10 signals for the Ad skeleton, and 81 signals out of 84 expected signals for the C_{84} cage at the sp^2 carbon region of 124−153 ppm, suggesting that the Ad addition caused the rupture of the C−C bond on the carbon cage to form a fulleroid structure. The similarity in the absorption spectra of pristine C_{84} and C_{84}(Ad)-A also shows good agreement with the fulleroid structure of C_{84}(Ad)-A because such a fulleroid retains its original π-electrons of the carbon cage (Figure 3).

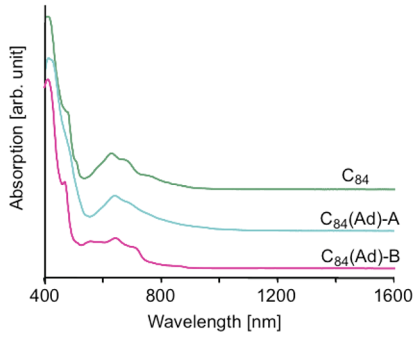

Figure 3. Absorption spectra of C_{84}, C_{84}(Ad)-A, and C_{84}(Ad)-B in CS_2.

The contribution of Ad carbene and diazoadamantane must be considered in the photoreaction of C_{84} with **1**. To assess the chemical reactivity of C_{84} toward diazoadamantane, photolysis of 5′,5′-dimethoxyspiro[adamantane]-2,2′-[Δ^3-1,3,4-oxadiazoline] (**2**) in the presence of C_{84} was conducted at −78 °C because **2** is known to give diazoadamantane exclusively under photoirradiation (Scheme 2).[14,15] On the one hand, photoirradiation to a toluene solution of **2** (0.16 equiv) followed by mixing with C_{84} at −78 °C caused the formation of C_{84}(Ad)-A and C_{84}(Ad)-B in a 10:1 ratio (yields: 4% and 0.3%, respectively, estimated from the HPLC peak area). On the other hand, photoirradiation to a toluene solution of **1** (0.16 equiv) followed by mixing with C_{84} at −78 °C caused the formation of C_{84}(Ad)-A and C_{84}(Ad)-B in a 10:1 ratio (yields: 8% and 0.8%, respectively, estimated from the HPLC peak area). In both cases, formation of the corresponding pyrazoline intermediate was not observed experimentally. Comparable product ratios between the reaction of C_{84} with **1** and that of C_{84} with **2** imply that in situ generated diazoadamantane contributes mainly to the reaction process in the photoreaction of C_{84} with **1**, although no conclusive evidence exists for the impossibility of Ad carbene addition on C_{84}.

Scheme 2. Reaction of C_{84} with 2 under Photoirradiation

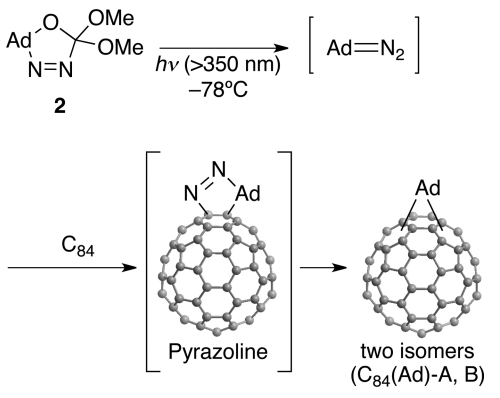

To assess the stability of the Ad adducts, we conducted photolysis of pure C_{84}(Ad)-A and C_{84}(Ad)-B by themselves. After 20 min of photoirradiation, no interconversion was observed between C_{84}(Ad)-A and C_{84}(Ad)-B under the photolytic conditions. However, it is particularly interesting that C_{84}(Ad)-A was interconverted to C_{84}(Ad)-B under heating at 80 °C. The quantitative thermal isomerization process was monitored using HPLC. After heating for 8 h, C_{84}(Ad)-A was consumed completely; C_{84}(Ad)-B was formed in 89% yield (estimated from the HPLC peak area). Similar thermal interconversion was also observed in Ad carbene adducts of La@C_{2v}(9)-C_{82}[12b] and Sc_2C_2@C_{2v}(5)-C_{80}.[16]

Mechanisms of the Ad Addition on C_{84} and the Interconversion of C_{84}(Ad) to C_{84}(Ad)-B. Density functional theory (DFT) calculations revealed that the 2-fold degenerate LUMO is localized primarily at the [6,6]-(a−a) bond in C_{84} (see inset in Figure 4).[17] In this respect, Diederich et al. reported that the (a−a) bond has the highest π-bond order.[18] Therefore, it is most likely that the regioselective [3 + 2] cycloaddition of C_{84} with diazoadamantane took place at the [6,6]-(a−a) bond to give the pyrazoline intermediate. In fact, a reasonable transition state (TS_{3+2}) was found, as shown in Figure 4. The energy barrier from the intermediate (INT_{3+2}) to TS_{3+2} is 5.1 kcal mol^{-1}. The 2-fold degenerate HOMO is not distributed to the [6,6]-(a−a) bond. The Ad carbene addition to such bonds must be unfavorable because Ad carbene is electrophilic.

Regarding the decomposition of the pyrazoline, two possible pathways must be considered (Figure 5) by analogy with reported examples of C_{60}-pyrazoline derivatives.[19] In a stepwise mechanism, the pyrazoline decomposition was initiated by the C−N bond cleavage under photoirradiation. After the subsequent N_2 extrusion, the resulting diradical intermediate engenders the [6,6]-(a−a)-closed methanofullerene and the [5,6]-(a−b)-closed fulleroid by subsequent radical coupling, of which the former corresponds to C_{84}(Ad)-B. However, according to DFT calculations, the stepwise pathway is unfavored in energy. The energy barrier is as large as 56.9 kcal mol^{-1}. Therefore, we infer that such a mechanism cannot take place as a major path. However, in a concerted [π^2s + π^2s + σ^2a + σ^2s] mechanism, the barrier to yield the [5,6]-(a−b)-closed fulleroid is 27.3 kcal mol^{-1}, which is 29.6 kcal mol^{-1} lower in energy than that of the stepwise mechanism. In this context, we concluded that the decomposition occurred via a concerted pathway. The resulting [5,6]-(a−b)-open fulleroid is expected to be C_{84}(Ad)-A.

As for the thermal interconversion of C_{84}(Ad)-A to C_{84}(Ad)-B, we found a reasonable transition state (TS_{iso}-concerted) in a concerted [1,5]-sigmatropic shift, as shown in Figure 6. The reaction barrier of the concerted isomerization from C_{84}(Ad)-A to C_{84}(Ad)-B is 32.6 kcal mol^{-1}. C_{84}(Ad)-B is 24.7 kcal mol^{-1} more stable than C_{84}(Ad)-A.

DOI: 10.1021/jacs.6b10751
J. Am. Chem. Soc. 2016, 138, 16523−16532

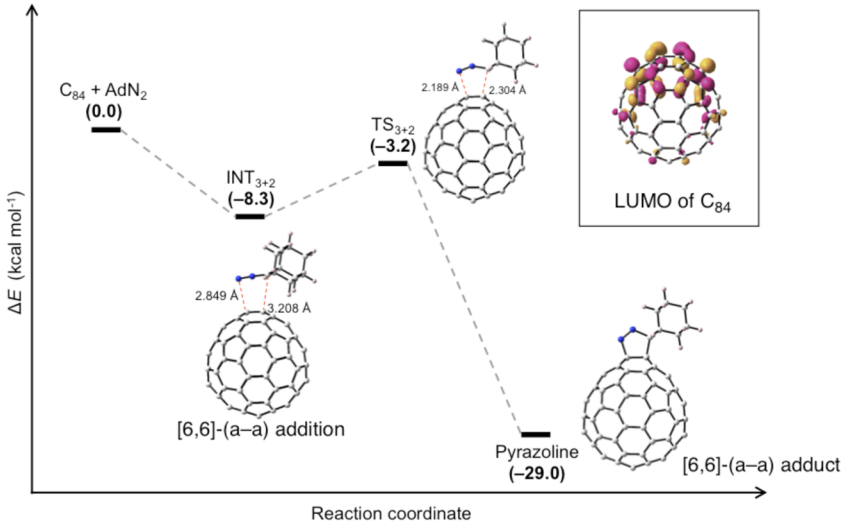

Figure 4. Energy profiles (in kcal mol^{-1}) for the [3 + 2] cycloaddition of C_{84} with in situ generated diazoadamantane (AdN_2) to form the pyrazoline intermediate. The inset shows LUMO of C_{84}.

Reactivity of Sc_2C_2@D_{2d}(23)-C_{84} and the Structure Determination of the Ad Adducts. Turning to Sc_2C_2@D_{2d}(23)-C_{84}, which we abbreviate as Sc_2C_2@C_{84}, photoirradiation to a toluene solution of Sc_2C_2@C_{84} in the presence of 50 equiv of **1** yielded four monoadducts in a 8:7:3:1 ratio after 60 s (Scheme 3). Subsequent HPLC separation afforded isolation of the monoadducts, designated as Sc_2C_2@C_{84}(Ad)-A, Sc_2C_2@C_{84}(Ad)-B, Sc_2C_2@C_{84}(Ad)-C, and Sc_2C_2@C_{84}(Ad)-D in order of decreasing yields. The absorption spectra of the four isomers are comparable to that of pristine Sc_2C_2@C_{84}, suggesting that all the monoadducts retain their π-electron systems and that they could have fulleroid structures rather than methanofullerene structures (Figure 7). The ^{13}C NMR spectra suggest that all three isomers of Sc_2C_2@C_{84}(Ad)-A, Sc_2C_2@C_{84}(Ad)-B, and Sc_2C_2@C_{84}(Ad)-C have C_1 symmetry, although the NMR data of Sc_2C_2@C_{84}(Ad)-D are lacking because of the insufficient amount of the sample. Among the four isomers, we obtained a single crystal of Sc_2C_2@C_{84}(Ad)-C suitable for XRD studies. Both the carbon cage and the encaged cluster are disordered. Nevertheless, the X-ray structure of Sc_2C_2@C_{84}(Ad)-C shows clearly that the addition took place at the (k–i′) bond between two six-membered rings (hereinafter, the bond is designated as a [6,6]-(k–i′) bond), forming a [6,6]-open fulleroid (Figure 8), in accord with the absorption spectroscopy. The C···C distance between the cage carbons bonded to the Ad moiety is 1.792 Å. The DFT calculations support the [6,6]-open fulleroid structure of Sc_2C_2@C_{84}(Ad)-C. The opened C···C separation was calculated as 1.664 Å, which shows agreement with the distance found in the X-ray structure. In the optimized structure, the ^{13}C chemical shifts of the cage carbons bonded to the Ad moiety were calculated as 85.12 and 96.37 ppm. The values agree well with the experimental values obtained at 88.01 and 98.72 ppm. The encaged Sc_2C_2 cluster was found in similar positions to those found in the cocrystals of pristine Sc_2C_2@C_{84} and cobalt octaethylporphyrin.[20]

We conducted the photochemical reaction of Sc_2C_2@C_{84} and **2**. However, no reaction proceeded. Results show that, unlike D_{2d}(23)-C_{84}, Sc_2C_2@C_{84} is not reactive toward diazoadamantane. Accordingly, we conclude that the photochemical reaction of Sc_2C_2@C_{84} and **1** proceeded via a carbene addition mechanism.

We also conducted photolysis of pure Sc_2C_2@C_{84}(Ad)-A and Sc_2C_2@C_{84}(Ad)-B by themselves. After 20 min of photoirradiation, we observed no interconversion under the photolytic conditions. Nevertheless, it is noteworthy that both Sc_2C_2@C_{84}(Ad)-A and Sc_2C_2@C_{84}(Ad)-B were interconverted respectively to Sc_2C_2@C_{84}(Ad)-C under heating at 100 °C.

Regioselectivity of Ad Addition on Sc_2C_2@C_{84}. As for the thermal interconversion of Sc_2C_2@C_{84}(Ad)-A and Sc_2C_2@C_{84}(Ad)-B to Sc_2C_2@C_{84}(Ad)-C, we speculate that the addend moves to bind with an adjacent bond, as proposed for the interconversion of empty C_{84}(Ad)-A to C_{84}(Ad)-B. Based on this hypothesis, the possible addition sites in Sc_2C_2@C_{84}(Ad)-A and Sc_2C_2@C_{84}(Ad)-B can be limited to (k–k), (k–f), (h′–i′), and (i′–j′).[21] The [6,6]-(k–k)-open, [6,6]-(k–f)-open, [5,6]-(h′–i′)-open, and [5,6]-(i′–j′)-open adducts are 6.2, 8.7, 16.1, and 16.0 kcal mol^{-1} higher in energy than the [6,6]-(k–i′)-open adduct that corresponds to Sc_2C_2@C_{84}(Ad)-C, as shown in Figure 9. Therefore, Sc_2C_2@C_{84}(Ad)-A and Sc_2C_2@C_{84}(Ad)-B could be the [6,6]-(k–k) and [6,6]-(k–f) addition products. However, we were unable to achieve final structural identification for Sc_2C_2@C_{84}(Ad)-A and Sc_2C_2@C_{84}(Ad)-B as well as that for Sc_2C_2@C_{84}(Ad)-D because one cannot deny the possibility of carbene transfer or a "walk on the sphere" rearrangement.[22]

Inspection of the MO diagrams shows that the LUMO of Sc_2C_2@C_{84} is higher in energy than that of C_{84} (Figure 10). In this context, the inertness of Sc_2C_2@C_{84} toward diazoadamantane can be inferred as resulting from the energy mismatch between their frontier orbitals. However, the reactivity of Sc_2C_2@C_{84} possessing the higher HOMO level because of the Sc_2C_2 doping could be higher than that of C_{84} toward the electrophilic Ad carbene. Nevertheless, the distribution of the HOMO is not an efficient criterion to predict the reactive sites on Sc_2C_2@C_{84} because the HOMO is delocalized over the hemisphere.

Next we examine the charge density and POAV values (Table 1) in the cage carbons. Results of our previous studies have pointed out that the favorable addition position in La@C_{2v}(9)-C_{82} is explainable based on these criteria in Ad carbene

DOI: 10.1021/jacs.6b10751
J. Am. Chem. Soc. 2016, 138, 16523–16532

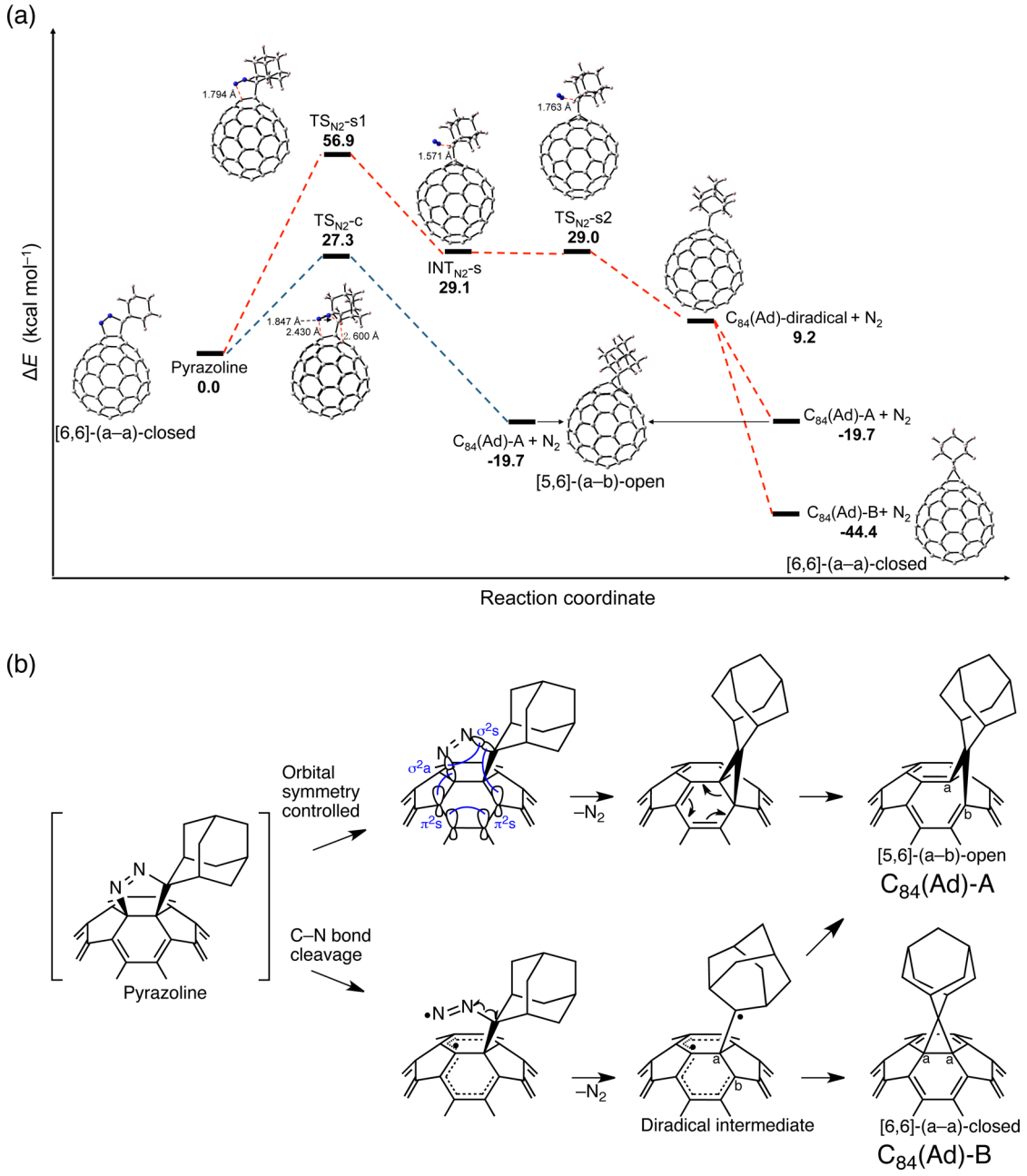

Figure 5. (a) Energy profiles (in kcal mol^{-1}) for the two plausible decomposition pathways (red shows the stepwise mechanism, blue shows the concerted mechanism) of the C_{84}-pyrazoline intermediate. (b) Schematic description of the decomposition pathways.

addition.[12a] Carbon atoms bearing high POAV values and high negative charge density tend to be most reactive toward Ad carbene. In $Sc_2C_2@C_{84}$, carbon atoms near the encaged Sc atoms such as C(a), C(b), C(c), and C(e) tend to have high negative charge densities. In addition, C(a) in $Sc_2C_2@C_{84}$ has higher POAV values than C(a) in C_{84}. However, C(k) and C(i), which are the addition site in $Sc_2C_2@C_{84}$(Ad)-C, have no high negative charge density. DFT calculations suggest that the [6,6]-(a–a)-open and [5,6]-(a–b)-open adducts are 6.3 and 9.7 kcal mol^{-1} higher in energy than $Sc_2C_2@C_{84}$(Ad)-C (see Figure 7). In this context, results suggest that the formation of $Sc_2C_2@C_{84}$(Ad)-C is governed by thermodynamic control rather than kinetic control.

CONCLUSION

In summary, we demonstrated that the reactivity of the $D_{2d}(23)$-C_{84} carbon cage in photoreaction with **1** is changed drastically by endohedral Sc_2C_2 doping. In the case of empty C_{84}, two Ad monoadducts were obtained in the photolysis of **1**. Single-crystal XRD investigations revealed that the minor isomer, C_{84}(Ad)-B, is the [6,6]-(a–a)-closed methanofullerene. Although single crystals of the major isomer, C_{84}(Ad)-A, were not obtained, isomerization studies and DFT calculations suggest that C_{84}(Ad)-A is the [5,6]-(a–b) open fulleroid. DFT calculations also provide the plausible reaction mechanism of Ad addition on C_{84}, showing that the initial [3 + 2] cycloaddition at the (a–a) bond with in situ generated diazoadamantane took place, followed by N_2 extrusion, to form a pyrazoline intermediate. Subsequent decomposition of

DOI: 10.1021/jacs.6b10751
J. Am. Chem. Soc. 2016, 138, 16523–16532

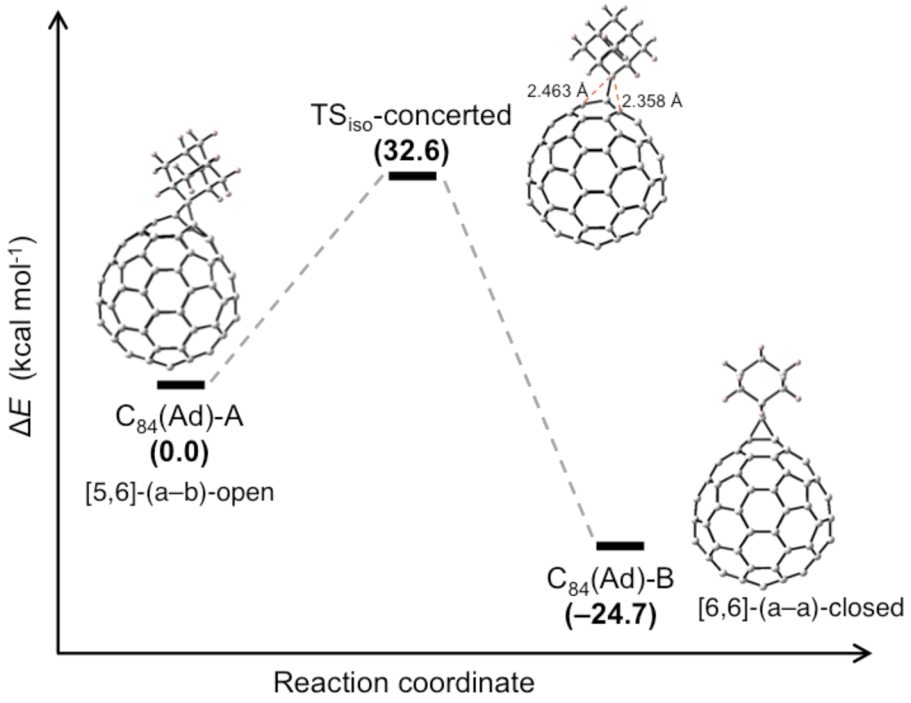

Figure 6. Energy profiles (in kcal mol^{-1}) for the concerted interconversion mechanism from C_{84}(Ad)-A to C_{84}(Ad)-B.

Scheme 3. Reaction of $Sc_2C_2@C_{84}$ with 1 under Photoirradiation

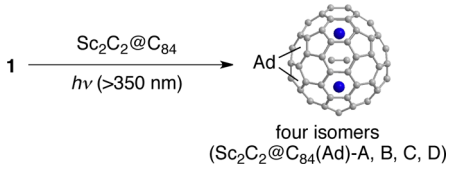

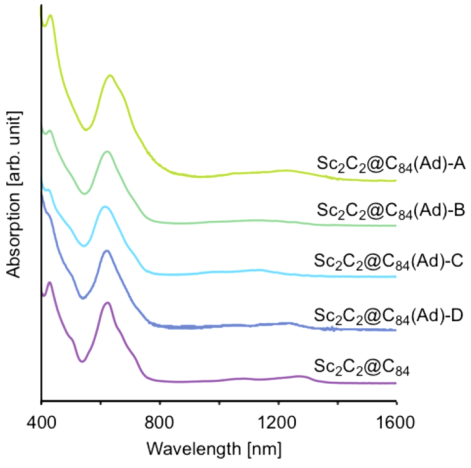

Figure 7. Absorption spectra of $Sc_2C_2@C_{84}$, $Sc_2C_2@C_{84}$(Ad)-A, $Sc_2C_2@C_{84}$(Ad)-B, $Sc_2C_2@C_{84}$(Ad)-C, and $Sc_2C_2@C_{84}$(Ad)-D in CS_2.

the pyrazoline via a concerted [π^2s + π^2s + σ^2a + σ^2s] pathway can afford the [5,6]-(a–b)-open fulleroid, C_{84}(Ad)-A, as the kinetic product. In addition, DFT calculations suggest that interconversion from C_{84}(Ad)-A to C_{84}(Ad)-B, which is thermodynamically favorable, took place via a [1,5]-sigmatropic shift. However, in the case of $Sc_2C_2@C_{84}$, four Ad monoadducts were obtained in the photolysis of **1**. Single-

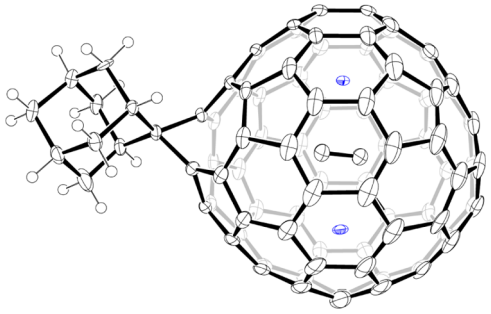

Figure 8. ORTEP drawing of $Sc_2C_2@C_{84}$(Ad)-C ([6,6]-(k–i′)-open fulleroid) with thermal ellipsoids shown at the 50% probability level for 90 K. Only the major cage orientation with 0.63 occupancy and the major Sc sites with 0.53 occupancy and the major C_2 sites with 0.69 occupancy are shown. Solvate molecules are omitted for clarity.

crystal XRD studies showed that the third most abundant isomer, $Sc_2C_2@C_{84}$(Ad)-C, is the [6,6]-(k–i′)-open fulleroid. Although we were unable to achieve final structural identification for the other isomers, $Sc_2C_2@C_{84}$(Ad)-A, $Sc_2C_2@C_{84}$(Ad)-B, and $Sc_2C_2@C_{84}$(Ad)-D, we found that $Sc_2C_2@C_{84}$(Ad)-A and $Sc_2C_2@C_{84}$(Ad)-B interconverted to $Sc_2C_2@C_{84}$(Ad)-C under thermal conditions. Based on the hypothesis that the addend moves to bind with an adjacent bond, the addition sites in $Sc_2C_2@C_{84}$(Ad)-A and $Sc_2C_2@C_{84}$(Ad)-B can be limited to four candidates. DFT calculations show that $Sc_2C_2@C_{84}$(Ad)-C is the most thermodynamically stable among the candidates. Based on the fact that $Sc_2C_2@C_{84}$ is not reactive toward in situ generated diazoadamantane, we conclude that the Ad addition to $Sc_2C_2@C_{84}$ proceeded via a carbene mechanism. DFT calculations suggest that raising the LUMO level by the Sc_2C_2 doping causes the inertness of $Sc_2C_2@C_{84}$ toward diazoadamantane. However, raising the HOMO level might become favorable for the addition of electrophilic Ad carbene to the carbon cage. Additional studies should be conducted to elucidate the structures of C_{84}(Ad)-A,

DOI: 10.1021/jacs.6b10751
J. Am. Chem. Soc. 2016, 138, 16523–16532

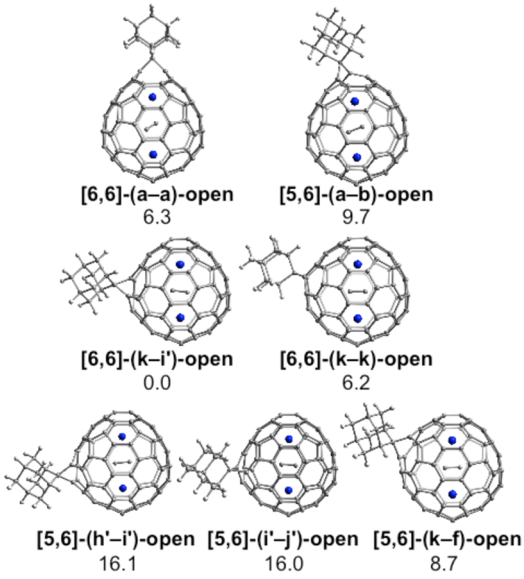

Figure 9. Optimized structures and relative energies (in kcal mol^{-1}) of seven selected Ad monoadducts of $Sc_2C_2@C_{84}$.

$Sc_2C_2@C_{84}$(Ad)-A, and $Sc_2C_2@C_{84}$(Ad)-B by single-crystal XRD and to explain the formation mechanism of C_{84}(Ad)-B and the regioselectivity in the reaction of $Sc_2C_2@C_{84}$ with Ad carbene.

EXPERIMENTAL SECTION

Reaction of C_{84} with 1 under Photoirradiation at Room Temperature. A toluene (2.0 mL) solution of C_{84} (0.050 mg, 5.0 × 10^{-5} mmol) and 47 equiv of **1** (0.38 mg, 2.3 × 10^{-3} mmol) was degassed by three freeze–pump–saw cycles under reduced pressure. The mixture was photoirradiated using an ultrahigh-pressure mercury-arc lamp through a cutoff filter (cutoff < 350 nm) at room temperature. After irradiation for 90 s, 52% of C_{84} was consumed. The monoadducts were isolated by recycling HPLC using a Buckyprep column to obtain pure C_{84}(Ad)-A and C_{84}(Ad)-B. The conversion yields of C_{84}(Ad)-A and C_{84}(Ad)-B were estimated as 80% and 12% using the HPLC peak area.

C_{84}(Ad)-A. ^{1}H NMR (500 MHz, CS_2/1,1,2,2-tetrachloroethane-d_2 1:1, 298 K) δ 5.12 (brs, 1H), 2.88 (brs, 1H), 2.78 (brd, J = 12.5 Hz, 1H), 2.30 (dd, J = 12.5, 2.0 Hz, 1H), 2.23–2.15 (m, 5H), 2.01 (brs, 1H), 1.95 (brd, J = 12.5 Hz, 1H), 1.89 (brs, 1H), 1.85 (dd, J = 12.5, 2.0 Hz, 1H), 1.80 ppm (brd, J = 9.0 Hz, 1H). ^{13}C NMR (125 MHz, CS_2/1,1,2,2-tetrachloroethane-d_2 1:1, 298 K) δ 152.50, 147.06, 145.56, 144.56, 144.19, 143.79, 143.67, 143.38, 142.96, 141.96, 141.87, 141.70, 141.66, 141.35, 141.34, 141.19, 140.77, 140.70, 140.64, 140.62, 140.57, 140.45, 140.26, 140.19, 140.15, 140.34, 140.08, 139.88, 139.86, 139.82, 139.75, 139.72, 139.67, 139.61, 139.34, 139.29, 139.25, 139.14, 139.01, 138.81, 138.72, 138.64, 138.60, 138.58, 138.52, 138.48, 138.47, 138.43, 138.39, 138.32, 137.92, 137.89, 137.84, 137.11, 136.98, 136.85, 136.72, 136.58, 136.53, 136.39, 136.29, 136.18, 135.89, 135.18, 135.00, 134.92, 134.55, 134.41, 134.35, 134.18, 134.14, 132.05, 132.01, 129.76, 129.60, 128.91, 128.83, 128.10, 127.58, 125.21, 124.74, 58.33, 37.45, 36.07, 35.19, 34.67, 34.07, 33.83, 33.34, 27.24, 26.81 ppm; 91 resonances out of 94 expected ones were observed. MALDI-TOF MS (matrix = 1,1,4,4-tetraphenyl-1,3-butadiene (TPB)) m/z 1142 [M$^-$].

C_{84}(Ad)-B. ^{1}H NMR (500 MHz, CS_2/1,1,2,2-tetrachloroethane-d_2 1:1, 298 K) δ 3.94 (brs, 2H), 2.56 (brd, J = 12.0 Hz, 4H), 2.41 (brs, 2H), 2.38 (brd, J = 12.0 Hz, 4H), 2.22 ppm (brs, 2H). ^{13}C NMR (125

Table 1. NBO Charge Density and POAV Values of Carbon Atoms in C_{84} (left) and $Sc_2C_2@C_{84}$ (right)

atom in C_{84}	charge density	POAV value	atom in $Sc_2C_2@C_{84}$	charge density	POAV value
a	0.022	10.78	a	−0.090	13.74
b	0.006	10.51	b	−0.082	10.01
c	−0.001	8.84	c	−0.020	8.77
d	0.001	10.55	d	−0.006	10.35
e	0.006	9.61	e	−0.045	8.18
f	−0.008	7.94	f	0.014	7.94
g	0.000	10.59	g	−0.007	11.40
h	0.002	10.98	h	−0.003	10.92
i	−0.005	10.86	i	0.006	10.90
j	0.007	10.72	j	−0.005	10.81
k	0.001	7.72	k	0.012	7.53
			a′	−0.093	13.95
			b′	−0.082	9.96
			c′	−0.016	8.84
			d′	−0.004	10.37
			e′	−0.052	8.10
			f′	0.009	7.82
			g′	−0.006	11.42
			h′	0.000	10.91
			i′	0.011	10.90
			j′	−0.002	10.83
			k′	0.005	7.44

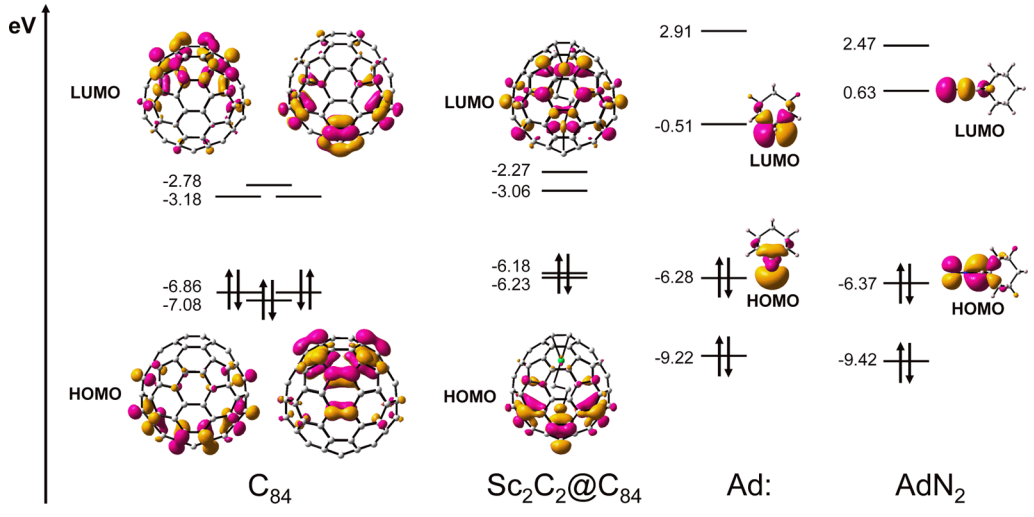

Figure 10. MO diagrams (isosurface = 0.03 au) of C_{84}, $Sc_2C_2@C_{84}$, Ad carbene (Ad:), and diazoadamantane (AdN_2).

DOI: 10.1021/jacs.6b10751
J. Am. Chem. Soc. 2016, 138, 16523–16532

MHz, CS_2/CD_2Cl_2 1:2, 298 K) δ 151.86, 144.61, 144.20, 143.62, 143.56, 143.03, 142.54, 141.85, 141.64, 139.77, 139.02, 138.99, 138.56, 138.46, 138.37, 138.13, 137.33, 135.67, 134.41, 68.86, 68.32, 39.49, 31.18, 30.62, 29.76, 24.62, 23.96 ppm; 27 resonances out of 29 expected ones were observed because of peak overlap. MALDI-TOF MS (matrix = TPB) m/z 1142 [M^-].

Crystal Data for C_{84}(Ad)-B. $C_{94}H_{14}\cdot 2(C_6H_4Cl_2)$, M_w = 1437.04, crystal size: 0.10 × 0.08 × 0.07 mm^3, monoclinic, $C2/c$, a = 44.997(18) Å, b = 11.379(4) Å, c = 22.258(9) Å, β = 90.415(7)°, V = 11348(8) $Å^3$, Z = 8, D_{calc} = 1.682 g/cm^3, μ = 0.278 mm^{-1}, T = 90 K, 47 430 reflections, 7936 unique reflections; 3646 with $I > 2\sigma(I)$; R_1 = 0.0474 [$I > 2\ \sigma(I)$], wR_2 = 0.1093 (all data), GOF (on F^2) = 0.766. The maximum residual electron density is equal to 0.512 e $Å^{-3}$. All measurements were obtained at beamline BL-8B of the Photon Factory, KEK, Japan. CCDC 1501207 includes the supplementary crystallographic data used for this Article.

*Reaction of C_{84} with **1** under Photoirradiation at −78 °C.* In a two-way Pyrex tube, a 1.0 mL toluene solution of C_{84} (0.040 mg, 4.0 × 10^{-5} mmol) was added to one side and a 1.0 mL toluene solution of **1** (0.0010 mg, 6.4 × 10^{-6} mmol) was added to the other side. The two solutions were degassed using three freeze−pump−thaw cycles under reduced pressures. The side tube containing a solution of **1** was photoirradiated using a ultrahigh-pressure mercury-arc lamp through a cutoff filter (cutoff < 300 nm) at −78 °C. After irradiation for 3 min, the solution of **1** was mixed with the solution of C_{84} in the other side. Then the mixture stood for 5−60 min at −78 °C, after which it was injected into an analytical HPLC, where the column was cooled to 0 °C in an ice bath. Yield: 8% (C_{84}(Ad)-A) and 0.8% (C_{84}(Ad)-B) accompanied by 26% consumption of C_{84} (estimated from the HPLC peak area). No other product was detected.

*Reaction of C_{84} with **2** under Photoirradiation at −78 °C.* In a two-way Pyrex tube, a 1.0 mL toluene solution of C_{84} (0.040 mg, 4.0 × 10^{-5} mmol) was added to one side; a 1.0 mL toluene solution of **2** (0.0014 mg, 5.8 × 10^{-6} mmol) was added to the other side. The two solutions were degassed using three freeze−pump−thaw cycles under reduced pressures. The side tube containing a solution of **2** was photoirradiated using an ultrahigh-pressure mercury-arc lamp through a cutoff filter (cutoff < 300 nm) at −78 °C. After irradiation for 3 min, the solution of **2** was mixed with the solution of C_{84} in the other side. Then the mixture stood for 5−60 min at −78 °C, after which it was injected into an analytical HPLC, where the column was cooled to 0 °C in an ice bath. Yield: 4% (C_{84}(Ad)-A) and 0.3% (C_{84}(Ad)-B) accompanied by 44% consumption of C_{84} (estimated from the HPLC peak area). No other product was detected.

Thermal Isomerization of C_{84}(Ad)-A to C_{84}(Ad)-B. A mixture of C_{84}(Ad)-A (2.5 μg, 2.2 × 10^{-6} mmol), toluene (200 μL), and C_{60} (50 μg, 6.9 × 10^{-5} mmol) as an internal reference was sealed in a Pyrex tube after degassing by three freeze−pump−thaw cycles. The tube was heated at 80 °C in an oil bath for 2−8 h. The solution was analyzed using analytical HPLC. Yield: 89% (C_{84}(Ad)-B) accompanied by 100% consumption of C_{84}(Ad)-A (estimated from the HPLC peak area). The formation of C_{84}(Ad)-B was also confirmed using a ^{13}C NMR measurement. Note that C_{60}(Ad) was not formed under the applied conditions.

Reaction of Sc_2C_2@C_{84} with 1 under Photoirradiation at Room Temperature. A toluene (2.0 mL) solution of Sc_2C_2@C_{84} (0.050 mg, 4.5 × 10^{-5} mmol) and 48 equiv of **1** (0.35 mg, 2.2 × 10^{-3} mmol) were degassed by three freeze−pump−thaw cycles under reduced pressure. The mixture was photoirradiated using an ultrahigh-pressure mercury-arc lamp through a cutoff filter (<350 nm) at room temperature. After irradiation for 90 s, 76% of Sc_2C_2@C_{84} was consumed. The monoadducts were isolated by recycling HPLC using a Buckyprep column to obtain pure Sc_2C_2@C_{84}(Ad)-A, Sc_2C_2@C_{84}(Ad)-B, Sc_2C_2@C_{84}(Ad)-C, and Sc_2C_2@C_{84}(Ad)-D. The conversion yields of Sc_2C_2@C_{84}(Ad)-A, Sc_2C_2@C_{84}(Ad)-B, Sc_2C_2@C_{84}(Ad)-C, and Sc_2C_2@C_{84}(Ad)-D were estimated from the HPLC peak area as 40%, 37%, 16%, and 5%.

Sc_2C_2@C_{84}(Ad)-A. ^{13}C NMR (125 MHz, CS_2/1,1,2,2-tetrachloroethane-d_2 1:1, 280 K) δ 151.32, 150.39, 149.13, 148.94, 148.78, 148.37, 148.20, 147.75, 147.58, 147.15, 146.90, 146.75, 146.53, 146.23, 145.68, 145.38, 145.23, 144.90, 144.70, 144.59, 144.10, 144.04, 143.86, 142.81, 142.73, 142.60, 142.81, 142.73, 142.60, 139.82, 139.52, 138.88, 138.54, 138.44, 138.15, 138.05, 139.91, 137.68, 137.63, 137.59, 137.48, 137.44, 136.98, 136.75, 136.60, 136.50, 136.48, 136.21, 136.07, 135.86, 135.58, 135.45, 135.24, 134.97, 134.71, 134.52, 134.41, 134.11, 133.27, 133.05, 132.85, 132.69, 132.47, 132.41, 131.59, 131.40, 131.32, 131.26, 131.02, 130.15, 129.61, 129.35, 128.85, 128.51, 128.13, 128.06, 127.27, 127.13, 125.91, 122.85, 67.69, 38.46, 34.37, 31.99, 30.25, 29.49, 28.87, 23.69, 23.16, 22.91 ppm; 90 resonances out of 95 expected ones were observed. Observation of a fine ^{1}H NMR spectrum and its signal assignment failed because of the poor solubility. MALDI-TOF MS (matrix = TPB) m/z 1256 [M^-].

Sc_2C_2@C_{84}(Ad)-B. ^{13}C NMR (125 MHz, CS_2/1,1,2,2-tetrachloroethane-d_2 1:1, 280 K) δ 149.74, 149.00, 148.62, 148.48, 148.35, 148.22, 148.16, 147.95, 147.83, 147.59, 147.53, 146.69, 145.55, 143.69, 143.45, 143.35, 143.19, 143.08, 143.00, 142.73, 142.16, 142.02, 141.59, 139.87, 139.68, 139.25, 138.61, 138.25, 138.09, 137.42, 137.37, 136.93, 136.81, 136.69, 136.59, 136.41, 136.29, 136.20, 135.89, 135.78, 135.49, 135.38, 135.23, 135.16, 134.52, 134.28, 134.14, 133.85, 132.40, 132.29, 132.19, 132.08, 131.84, 131.43, 141.33, 131.04, 130.44, 130.23, 130.06, 129.90, 1229.68, 129.00, 128.60, 128.53, 128.48, 128.11, 127.49, 127.32, 127.06, 126.77, 124.24, 123.55, 62.20, 43.06, 32.00, 29.51, 27.55, 27.16, 26.97, 26.54, 22.94, 21.44 ppm; 82 resonances out of 95 expected ones were observed. Observation of a fine ^{1}H NMR spectrum and its signal assignment failed because of the poor solubility of the sample. MALDI-TOF MS (matrix = TPB) m/z 1256 [M^-].

Sc_2C_2@C_{84}(Ad)-C. ^{1}H NMR (500 MHz, CS_2/1,1,2,2-tetrachloroethane-d_2 1:1, 298 K) δ 5.11 (brs, 1H), 2.88 (brs, 1H), 2.77 (brd, J = 13.5 Hz, 1H), 2.29 (brd, J = 12.5 Hz, 1H), 2.21 (brd, J = 13.5 Hz, 1H), 2.16 (brs, 4H), 2.01 (brs, 1H), 1.95 (brd, J = 13.5 Hz, 1H), 1.89 (brs, 1H), 1.85 (brd, J = 12.5 Hz, 1H), 1.80 ppm (brd, J = 9.5 Hz,1H) ; ^{13}C NMR (125 MHz, CS_2 (acetone-d_6 in capillary), 298 K) δ 151.16, 151.13, 150.35, 150.19, 149.97, 148.88, 148.97, 148.65, 148.51, 147.96, 147.41, 146.96, 146.51, 146.30, 146.03, 145.91, 145.85, 145.18, 144.91, 144.75, 144.69, 144.27, 144.25, 144.14, 143.79, 143.05, 142.43, 142.31, 142.16, 139.96, 139.86, 139.77, 139.25, 139.08, 138.91, 138.78, 138.68, 138.60, 138.28, 138.13, 137.92, 137.85, 137.70, 137.62, 137.60, 137.48, 137.41, 137.36, 136.74, 136.50, 136.08, 135.94, 135.26, 135.17, 135.14, 134.76, 133.93, 133.87, 133.74, 132.71, 132.55, 132.17, 132.08, 131.96, 131.00, 130.90, 130.74, 130.56, 130.32, 130.19, 129.98, 129.59, 129.50, 129.12, 129.08, 98.72, 88.01, 48.86, 37.12, 35.87, 35.35, 35.00, 34.27, 32.49, 28.14, 28.00, 27.95 ppm; 87 resonances out of 95 expected ones were observed. MALDI-TOF MS (matrix = TPB) m/z 1256 [M^-].

Crystal Data for Sc_2C_2@C_{84}(Ad)-C. $Sc_2C_{96}H_{14}\cdot 0.94(C_6H_4Cl_2)\cdot 0.66(CS_2)$, M_w = 1442.71, crystal size: 0.406 × 0.238 × 0.070 mm^3, triclinic, $P\bar{1}$, a = 11.2973(2) Å, b = 14.9219(3) Å, c = 16.4784(3) Å, α = 89.0570(10)°, β = 76.5460(10)°, γ = 74.1120(10)°, V = 2595.13(9) $Å^3$, Z = 2, D_{calc} = 1.846 g/cm^3, μ = 0.482 mm^{-1}, T = 90 K, 57 475 reflections, 18 721 unique reflections; 15 661 with $I > 2\sigma(I)$; R_1 = 0.0848 [$I > 2\ \sigma(I)$], wR_2 = 0.2430 (all data), GOF (on F^2) = 1.033. The maximum residual electron density is equal to 1.573 e $Å^{-3}$. All measurements were performed at beamline BL-8B of the Photon Factory, KEK, Japan. CCDC 1501208 includes the supplementary crystallographic data used for this Article.

*Reaction of S_2C_2@C_{84} with **2** under Photoirradiation at −78 °C.* In a two-way Pyrex tube, a 1.0 mL toluene solution of Sc_2C_2@C_{84} (0.040 mg, 3.6 × 10^{-5} mmol) was added to one side; a 1.0 mL toluene solution of **2** (0.0014 mg, 5.8 × 10^{-6} mmol) was added to the other side. The two solutions were degassed using three freeze−pump−thaw cycles under reduced pressures. The side tube containing **2** was photoirradiated using an ultrahigh-pressure mercury-arc lamp through a cutoff filter (cutoff < 300 nm) at −78 °C. After irradiation for 3 min, the solution of **2** was mixed with the solution of C_{84} in the other side; the mixture was left to stand for 5−60 min at −78 °C, after which it was injected into an analytical HPLC, where the column was cooled to 0 °C in an ice bath. The reaction mixture was further photoirradiated for 20 min and was injected into an analytical HPLC instrument. As a result, the HPLC analysis revealed no formation of products. The starting Sc_2C_2@C_{84} was not consumed.

DOI: 10.1021/jacs.6b10751
J. Am. Chem. Soc. 2016, 138, 16523−16532

Thermal Isomerization of Sc_2C_2@C_{84}(Ad)-A to Sc_2C_2@C_{84}(Ad)-C. A mixture of Sc_2C_2@C_{84}(Ad)-A (20 μg, 1.6×10^{-5} mmol), toluene (900 μL), and C_{60} (400 μg, 5.6×10^{-4} mmol) as an internal reference was sealed in a Pyrex tube after degassing by three freeze–pump–thaw cycles. The tube was heated at 100 °C in an oil bath for 4–11 h. The solution was then analyzed using analytical HPLC. C_{60}(Ad) was not formed under the applied conditions. Yield: 21% (Sc_2C_2@C_{84}(Ad)-B) accompanied by 52% consumption of Sc_2C_2@C_{84}(Ad)-A (estimated from the HPLC peak area).

Thermal Isomerization of Sc_2C_2@C_{84}(Ad)-B to Sc_2C_2@C_{84}(Ad)-C. A mixture of Sc_2C_2@C_{84}(Ad)-B (20 μg, 1.6×10^{-5} mmol), toluene (900 μL), and C_{60} (400 μg, 5.6×10^{-4} mmol) as an internal reference was sealed in a Pyrex tube after degassing by three freeze–pump–thaw cycles. The tube was heated at 100 °C in an oil bath for 24–96 h. The solution was analyzed using analytical HPLC. C_{60}(Ad) was not formed under these conditions. Yield: 65% (Sc_2C_2@C_{84}(Ad)-B) accompanied by 61% consumption of Sc_2C_2@C_{84}(Ad)-A (estimated from the HPLC peak area).

Calculations. All calculations were conducted using the Gaussian 09[23] program. Geometry optimization and vibrational frequency analyses were performed with density functional theory (DFT) at the dispersion-corrected M06-2X-GD3[24] level using the Lanl2DZ basis set and effective core potential[25] for Sc and the 6-31G(d)[26] basis set for C. Zero-point corrected values were used to draw energy profiles. NBO charge densities[27] and POAV values[13] were calculated at optimized geometries. For the calculations of ^{13}C chemical shifts, the larger 6-311G+(d,p) basis set was used for C.

■ ASSOCIATED CONTENT

Supporting Information

The Supporting Information is available free of charge on the ACS Publications website at DOI: 10.1021/jacs.6b10751.

Materials, along with experimental and computational details (PDF)

Crystallographic data (CIF, CIF)

■ AUTHOR INFORMATION

Corresponding Author

*akasaka@tara.tsukuba.ac.jp

ORCID

Takeshi Akasaka: 0000-0002-4073-4354

Present Addresses

[¶]Research Center for Advanced Science and Technology, The University of Tokyo, Tokyo 153-8904, Japan.

[△]Department of Chemistry, Faculty of Science, Josai University, Saitama 350-0295, Japan.

Notes

The authors declare no competing financial interest.

■ ACKNOWLEDGMENTS

This work was supported by a Grant-in-Aid for Scientific Research on Innovative Areas (No. 20108001, "pi-Space"), a Grant-in-Aid for Scientific Research (A) (No. 202455006) and (B) (No. 24350019), and Specially Promoted Research (No. 22000009) from the Ministry of Education, Culture, Sports, Science, and Technology of Japan.

■ REFERENCES

(1) (a) Chaur, M. N.; Melin, F.; Ortiz, A. L.; Echegoyen, L. *Angew. Chem., Int. Ed.* **2009**, *48*, 7514–7538. (b) Popov, A. A.; Yang, S.; Dunsch, L. *Chem. Rev.* **2013**, *113*, 5989–6113.

(2) (a) Yamada, M.; Akasaka, T. *Bull. Chem. Soc. Jpn.* **2014**, *87*, 1289–1314. (b) Nagase, S. *Bull. Chem. Soc. Jpn.* **2014**, *87*, 167–195. (c) Iiduka, Y.; Ikenaga, O.; Sakuraba, A.; Wakahara, T.; Tsuchiya, T.; Maeda, Y.; Nakahodo, Y.; Akasaka, T.; Kako, M.; Mizorogi, N.; Nagase, S. *J. Am. Chem. Soc.* **2005**, *127*, 9956–9957. (d) Kako, M.; Inaba, D.; Minami, K.; Iida, R.; Nakahodo, T.; Akasaka, T. *Heteroat. Chem.* **2014**, *25*, 584–591.

(3) Maeda, Y.; Miyashita, J.; Hasegawa, T.; Wakahara, T.; Tsuchiya, T.; Nakahodo, T.; Akasaka, T.; Mizorogi, N.; Kobayashi, K.; Nagase, S.; Kato, T.; Ban, N.; Nakajima, H.; Watanabe, Y. *J. Am. Chem. Soc.* **2005**, *127*, 12190–12191.

(4) Ge, Z.; Duchamp, J. C.; Cai, T.; Gibson, H. W.; Dorn, H. C. *J. Am. Chem. Soc.* **2005**, *127*, 16292–16298.

(5) In a related work, Kokubo et al. reported that Li^+@C_{60} reacted with cyclohexadiene about 2400 times faster than empty C_{60}: Ueno, H.; Kawakami, H.; Nakagawa, K.; Okada, H.; Ikuma, N.; Aoyagi, S.; Kokubo, K.; Matsuo, Y.; Oshima, T. *J. Am. Chem. Soc.* **2014**, *136*, 11162–11167.

(6) (a) Kikuchi, K.; Nakahara, N.; Wakabayashi, T.; Suzuki, S.; Shiromaru, H.; Miyake, Y.; Saito, K.; Ikemoto, I.; Kainosho, M.; Achiba, Y. *Nature* **1992**, *357*, 142–145. (b) Manolopoulos, D. E.; Fowler, P. W.; Taylor, R.; Kroto, H. W.; Walton, D. R. M. *J. Chem. Soc., Faraday Trans.* **1992**, *88*, 3117–3118. (c) Dennis, T. J. S.; Shinohara, H. *Chem. Commun.* **1998**, 619–620. (d) Balch, A. L.; Ginwalla, A. S.; Lee, J. W.; Noll, B. C.; Olmstead, M. M. *J. Am. Chem. Soc.* **1994**, *116*, 2227–2228.

(7) (a) Wang, C.-R.; Kai, T.; Tomiyama, T.; Yoshida, T.; Kobayashi, Y.; Nishibori, E.; Takata, M.; Sakata, M.; Shinohara, H. *Angew. Chem., Int. Ed.* **2001**, *40*, 397–399. (b) Yamazaki, Y.; Nakajima, K.; Wakahara, T.; Tsuchiya, T.; Ishitsuka, M. O.; Maeda, Y.; Akasaka, T.; Waelchli, M.; Mizorogi, N.; Nagase, S. *Angew. Chem., Int. Ed.* **2008**, *47*, 7905–7908.

(8) Yamada, M.; Akasaka, T.; Nagase, S. *Chem. Rev.* **2013**, *113*, 7209–7264.

(9) Akasaka, T.; Liu, M. T. H.; Niino, Y.; Maeda, Y.; Wakahara, T.; Okamura, M.; Kobayashi, K.; Nagase, S. *J. Am. Chem. Soc.* **2000**, *122*, 7134–7135.

(10) Bonneau, R.; Liu, M. T. H. *J. Am. Chem. Soc.* **1996**, *118*, 7229–7230.

(11) Wakahara, T.; Niino, Y.; Kato, T.; Maeda, Y.; Akasaka, T.; Liu, M. T. H.; Kobayashi, K.; Nagase, S. *J. Am. Chem. Soc.* **2002**, *124*, 9465–9468.

(12) (a) Maeda, Y.; Matsunaga, Y.; Wakahara, T.; Takahashi, S.; Tsuchiya, T.; Ishitsuka, M. O.; Hasegawa, T.; Akasaka, T.; Liu, M. T. H.; Kokura, K.; Horn, E.; Yoza, K.; Kato, T.; Okubo, S.; Kobayashi, K.; Nagase, S.; Yamamoto, K. *J. Am. Chem. Soc.* **2004**, *126*, 6858–6859. (b) Matsunaga, Y.; Maeda, Y.; Wakahara, T.; Tsuchiya, T.; Ishitsuka, M. O.; Akasaka, T.; Mizorogi, N.; Kobayashi, K.; Nagase, S.; Kadish, K. M. *ITE Lett. Batteries, New Technol. Med.* **2006**, *7*, 43–49.

(13) (a) Haddon, R. C. *Science* **1993**, *261*, 1545–1550. (b) Haddon, R. C. *J. Am. Chem. Soc.* **1997**, *119*, 1797–1798.

(14) Pezacki, J. P.; Wood, P. D.; Gadosy, T. A.; Lusztyk, J.; Warkentin, J. *J. Am. Chem. Soc.* **1998**, *120*, 8681–8691.

(15) Niino, Y.; Wakahara, T.; Akasaka, T.; Liu, M. T. H.; Kobayashi, K.; Nagase, S. *ITE Lett. Batteries, New Technol. Med.* **2002**, *3*, 82–85.

(16) Kurihara, H.; Lu, X.; Iiduka, Y.; Nikawa, H.; Mizorogi, N.; Slanina, Z.; Tsuchiya, T.; Nagase, S.; Akasaka, T. *J. Am. Chem. Soc.* **2012**, *134*, 3139–3144.

(17) (a) Nagase, S.; Kobayashi, K. *Chem. Phys. Lett.* **1994**, *231*, 319–324. (b) Boulas, P.; Jones, M. T.; Kadish, K. M.; Ruoff, R. S.; Lorents, D. C.; Tse, D. S. *J. Am. Chem. Soc.* **1994**, *116*, 9393–9394. (c) Dang, J.-S.; Wang, W.-W.; Zhao, X.; Nagase, S. *Org. Lett.* **2014**, *16*, 170–173.

(18) Crassous, J.; Rivera, J.; Fender, N. S.; Shu, L.; Echegoyen, L.; Thilgen, C.; Herrmann, A.; Diederich, F. *Angew. Chem., Int. Ed.* **1999**, *38*, 1613–1617.

(19) (a) Haldimann, R. F.; Klärner, F.-G.; Diederich, F. *Chem. Commun.* **1997**, 237–238. (b) Schick, G.; Hirsch, A. *Tetrahedron* **1998**, *54*, 4283–4296.

(20) Kurihara, H.; Lu, X.; Iiduka, Y.; Nikawa, H.; Hachiya, M.; Mizorogi, N.; Slanina, Z.; Tsuchiya, T.; Nagase, S.; Akasaka, T. *Inorg. Chem.* **2012**, *51*, 746–750.

DOI: 10.1021/jacs.6b10751
J. Am. Chem. Soc. 2016, 138, 16523–16532

(21) Rotation of the C_2 unit makes the molecular symmetry of $Sc_2C_2@C_{84}$ D_{2d} symmetric. Therefore, it is unnecessary to distinguish carbon atoms a−k from a′−k′ in the discussion. In fact, a subtle difference exists between them in charge densities and POAV values.
(22) Kessinger, R.; Gómez-López, M.; Boudon, C.; Gisselbrecht, J.-P.; Gross, M.; Echegoyen, L.; Diederich, F. *J. Am. Chem. Soc.* **1998**, *120*, 8545−8546.
(23) Frisch, M. J.; Trucks, G. W.; Schlegel, H. B.; Scuseria, G. E.; Robb, M. A.; Cheeseman, J. R.; Scalmani, G.; Barone, V.; Mennucci, B.; Petersson, G. A.; Nakatsuji, H.; Caricato, M.; Li, X.; Hratchian, H. P.; Izmaylov, A. F.; Bloino, J.; Zheng, G.; Sonnenberg, J. L.; Hada, M.; Ehara, M.; Toyota, K.; Fukuda, R.; Hasegawa, J.; Ishida, M.; Nakajima, T.; Honda, Y.; Kitao, O.; Nakai, H.; Vreven, T.; Montgomery, J. A., Jr.; Peralta, J. E.; Ogliaro, F.; Bearpark, M.; Heyd, J. J.; Brothers, E.; Kudin, K. N.; Staroverov, V. N.; Kobayashi, R.; Normand, J.; Raghavachari, K.; Rendell, A. J.; Burant, C.; Iyengar, S. S.; Tomasi, J.; Cossi, M.; Rega, N.; Millam, J. M.; Klene, M.; Knox, J. E.; Cross, J. B.; Bakken, V.; Adamo, C.; Jaramillo, J.; Gomperts, R.; Stratmann, R. E.; Yazyev, O.; Austin, A. J.; Cammi, R.; Pomelli, C.; Ochterski, J. W.; Martin, R. L.; Morokuma, K.; Zakrzewski, V. G.; Voth, G. A.; Salvador, P.; Dannenberg, J. J.; Dapprich, S.; Daniels, A. D.; Farkas, O.; Foresman, J. B.; Ortiz, J. V.; Cioslowski, J.; Fox, D. J. *Gaussian 09*, revision D.01; Gaussian, Inc.: Wallingford, CT, 2009.
(24) Zhao, Y.; Truhlar, D. G. *Theor. Chem. Acc.* **2008**, *120*, 215−241.
(25) Hay, P. J.; Wadt, W. R. *J. Chem. Phys.* **1985**, *82*, 299−310.
(26) Hehre, W. J.; Ditchfield, R.; Pople, J. A. *J. Chem. Phys.* **1972**, *56*, 2257−2261.
(27) Reed, A. E.; Weinstock, R. B.; Weinhold, F. *J. Chem. Phys.* **1985**, *83*, 735−746.

DOI: 10.1021/jacs.6b10751
J. Am. Chem. Soc. 2016, 138, 16523−16532